scientific reports

Check for updates

OPEN

Functional and genomic characterization of polyethylene degrading yeast *Meyerozyma carpophila* M6.0.2 isolated from marine plastic debris in East Java Indonesia

Nur Hidayatul Alami[1,5], Zahra Rahayu Puteri[2], Takehiro Esaki[3]✉, Yuichi Sugai[3], Fenryco Pratama[4], Isty Adhitya Purwasena[4]✉ & Pingkan Aditiawati[4]✉

Polyethylene (PE) is a primary contributor to environmental plastic pollution, posing a critical risk to ecosystems and living organisms. This study screened six yeast strains (BI.4.1.1, K3.1.2, M.5.0.1, M.5.0.3, M.6.0.1, and M.6.0.2) isolated from marine plastic debris in East Java, Indonesia, for their ability to degrade PE. Among these, *Meyerozyma carpophila* M6.0.2 demonstrated functional characteristics with the highest polyethylene-degrading activity in liquid medium after a 10-day incubation, with a degradation percentage of 0.4923%. This was supported by its biofilm-forming capacity, biosurfactant production, and broad metabolic activity as demonstrated by EcoPlate assays. In addition, Scanning Electron Microscope (SEM) and Fourier Transform Infrared Spectroscopy (FTIR) analyses of PE films revealed morphological changes and emergence of new peaks, respectively. Whole-genome sequencing (WGS) of strain M6.0.2 was performed using the Illumina NextSeq 2000 platform (PE 150), yielding a genome assembly of 10.34 Mb across 108 contigs with an N50 length of 1.08 Mb. A total of 5,352 putative genes were predicted. These findings highlight *Meyerozyma carpophila* M6.0.2 as a promising candidate for bioremediation of marine plastic pollution, emphasizing the combination of functional and genomic insights for a better understanding of the mechanism of PE biodegradation.

Keywords Biodegradation, Marine, Plastic, Polyethylene, Waste, Yeast

Plastic pollution constitutes a global environmental crisis that poses a significant threat to ecosystems, particularly marine environments[1]. Its persistent characteristics allow it to accumulate over a very long period, causing severe ecological effects, including impacts on biodiversity and human health[2,3]. Polyethylene (PE) is one of the primary polymers contributing to environmental plastic pollution, accounting for approximately 64% of all plastic materials[4–6]. It consists of long, linear ethylene monomers (C_2H_4)n chains. PE's highly stable aliphatic backbone renders it resistant to degradation and environmentally recalcitrant[7,8].

Indonesia has been reported as the second-largest producer of marine plastic waste after China. Studies conducted between 2015 and 2019 estimated that plastic debris entering the Indonesian marine environment ranged from 0.27 to 1.29 million tons per year[9,10]. Plastics such as PE can also fragment into microplastics

[1]Doctoral Program of Biology, School of Life Sciences and Technology, Institut Teknologi Bandung, Jl. Ganesha No. 10, Bandung 40132, Indonesia. [2]Master's Program in Biotechnology, School of Life Sciences and Technology, Institut Teknologi Bandung, Jl. Ganesha No. 10, Bandung 40132, Indonesia. [3]Department of Earth Resources Engineering, Faculty of Engineering, Kyushu University, 744 Motooka, Nishi-ku, Fukuoka 819-0395, Japan. [4]Microbial Biotechnology Research Group, School of Life Sciences and Technology, Institut Teknologi Bandung, Jl. Ganesha No.10, Bandung 40132, Indonesia. [5]Department of Biology, Faculty of Science and Data Analytics, Institut Teknologi Sepuluh Nopember, Jl. Raya ITS, Keputih, Sukolilo, Surabaya 60111, Indonesia. ✉email: esaki.takehiro.684@m.kyushu-u.ac.jp; isty@itb.ac.id; pingkan@itb.ac.id

and nanoplastics, which are increasingly recognized for their potential to harm marine organisms and transfer through food webs, raising concerns for human health[11].

PE waste represents one of the most pressing environmental challenges. Several strategies have been developed to enhance PE degradation, including photodegradation, thermo-oxidative degradation, and biodegradation. Compared with photo-physical degradation methods, biodegradation is more efficient, economical, and environmentally friendly[12–14]. Photodegradation, for instance, is a relatively slow process that may take up to two years. Photodegradation is associated with ultraviolet radiation, while thermal degradation leads to the decomposition of polyethylene with energy input from high temperatures. This significantly increases energy and operational costs. Both photodegradation and thermo-oxidative degradation can produce toxic gases such as dioxins ($C_4H_8O_2$), carbon monoxide (CO), hydrogen sulfide (H_2S), Polycyclic Aromatic Hydrocarbons (PAH), and furans (C_4H_4O), posing potential health hazards. Biodegradation is considered a more sustainable alternative due to its environmentally friendly nature and the absence of toxic by-products. It involves several enzymes produced by microorganisms that can degrade PE until it is completely mineralized[15,16].

Research on polyethylene (PE) degradation has predominantly focused on microorganisms from bacterial and fungal groups; however, studies involving yeast for plastic degradation, including PE, remain limited[17,18]. Similar to other fungi, marine yeasts—or yeasts isolated from marine environments—can adapt and survive under extreme conditions. Yeasts with this feature may be valuable for application in ex-situ processing of marine plastic waste using bioreactors[19]. These adaptive traits may not be present in terrestrial yeasts[20]. Many yeasts are known to produce extracellular enzymes and to form biofilms enclosed within an extracellular matrix[21,22]. In addition, they can produce biosurfactants, which can enhance cell attachment to plastic surfaces during biofilm formation. Improved cell adhesion to PE is expected to facilitate the degradation of this highly recalcitrant polymer[23].

Among the existing yeast taxa, the species *Meyerozyma carpophila* is widely distributed across various habitats, ranging from insects to estuarine environments. No studies have reported its role in PE degradation. To the best of our knowledge, the only existing studies within the genus *Meyerozyma* that report PE-degrading activity involve the species *Meyerozyma caribbica* and *Meyerozyma guilliermondii*[18,24].

As the specific mechanism of PE biodegradation remains unclear, many studies have investigated PE degradation by referring to the alkane biodegradation pathway, due to the chemical similarity between alkanes and PE. Several microbial enzymes are believed to play important roles in alkane degradation. Seo et al.[25] proposed a PE degradation mechanism involving P450 monooxygenase and hydroxylase as key initiating enzymes. In addition, enzymes such as laccase, peroxidase, alkane monooxygenase, hydroxylase, alcohol dehydrogenase, aldehyde dehydrogenase, esterase and lipase are thought to be involved in PE decomposition. However, further research is required to confirm the presence of functional genes directly or indirectly involved in PE degradation in yeast. Whole genome sequencing (WGS) enables the identification of specific genes and enzymes that may play a role in this process.

In plastic-polluted environments, microbes capable of degrading plastic can be found, as they have adapted to survive by utilizing plastic as a carbon source[26]. A previous study by Alami et al.[27] successfully isolated yeast strains from plastic waste biofilms collected in various plastic-contaminated locations in Surabaya and Banyuwangi, East Java, Indonesia. Out of 19 isolates obtained, six isolates—namely BI.4.1.1, K3.1.2, M.5.0.1, M.5.0.3, M.6.0.1, and M.6.0.2—were derived from plastic sampling sites in the marine environment (coastal area). A polyethylene-based media screening assay was performed to assess their ability to form clear zones. However, their potential for polyethylene degradation has not been fully characterized.

In this study, six yeast isolates obtained from marine plastic debris were investigated for their potential to degrade polyethylene (PE). The research aimed to comprehensively characterize the most promising isolate through phenotypic, biochemical, and genomic approaches. These included assessments of biofilm formation, biosurfactant production, and metabolic capabilities, as well as genome sequencing to identify candidate genes potentially involved in PE degradation.

To the best of our knowledge, this is the first report to explore the PE degrading ability of *M. carpophila*, particularly from a marine environment, and the first to integrate functional and genomic analysis of this species. Our findings provide new insights into the bioremediation potential of marine-derived yeast for addressing PE pollution.

Materials and methods

Plastic material

Three forms of polyethylene (PE)—powder, film, and granules—were employed in this study, each selected for its suitability to a specific experimental assay. PE powder (CAS No. 9002-88-4; Sigma-Aldrich, USA) was used for qualitative assays on solid media, including microbial growth and clear zone formation, owing to its ability to float on the agar surface during solidification, thereby facilitating direct substrate–microbe interactions[28]. A high-density polyethylene (HDPE) film (5 × 5 mm, 10 µm thick), sourced from packaging material purchased in Surabaya, Indonesia, was used in biofilm formation assays. Its thin profile and relatively large surface area made it well-suited for supporting microbial attachment and growth[29]. Low-density polyethylene (LDPE) granules (melt index: 190 °C/2.16 kg; Sigma-Aldrich, USA) were used for quantitative biodegradation assays in liquid media, as their uniform size and shape allow for accurate measurement of weight loss and enable subsequent surface and chemical structure analysis using Scanning Electron Microscopy (SEM) and Fourier Transform Infrared (FTIR) spectroscopy[30]. The PE powder and granules were sterilized by immersion in 70% ethanol for 2 h, followed by oven drying at 50 °C until a constant weight was achieved, and exposure to UV light for 1 hour[11]. The PE film was sterilized by immersion in 70% ethanol for 20 min and air-dried before use[31].

Yeast isolates

The yeast isolates used in this study—BI.4.1.1, K3.1.2, M5.0.1, M5.0.3, M6.0.1, and M6.0.2—have been deposited in the Airlangga University Culture Collection (AUCC), Surabaya, Indonesia, under the accession numbers UACC 365233 (M6.0.1), UACC 465223 (K3.1.2), UACC4 65224 (M5.0.1), UACC 465225 (M5.0.3), UACC 465226 (M6.0.2), and UACC 465227 (BI.4.1.1). These isolates were obtained from marine plastic debris collected from plastic-polluted areas in Surabaya and Banyuwangi, East Java, Indonesia. Subculturing of these isolates was performed on Wickerham's YM medium, composed of (per L): 3 g yeast extract, 3 g malt extract, 5 g peptone, 10 g glucose, and 20 g agar, prepared in seawater[32].

Yeast characterization and identification

A colony grown on Wickerham's YM medium for 2 days at room temperature (26 °C) was characterized based on macroscopic and microscopic morphological characteristics. Macroscopic characterization included texture, color, elevation, surface, and margin, while microscopic cellular characteristics were examined at 100× magnification using a binocular light microscope (model SE; Nikon Corporation, Tokyo, Japan) after staining with Lactophenol Cotton Blue. Cell shape and asexual reproduction were observed. In addition to morphological observation, molecular identification was performed for six yeast isolates. Four isolates (M5.0.1, BI.4.1.1, M5.0.3, and M6.0.2) were processed by Macrogen Inc. (Seoul, South Korea) for ITS sequencing. Isolates M5.0.1 and BI.4.1.1 were amplified using ITS1 (5′-TCCGTAGGTGAACCTGCG G-3′) and ITS4 (5′-TCCTCC GCTTATTGATATGC-3′), while isolates M5.0.3 and M6.0.2 were amplified using ITS5 (5′-GGAAGTAAAAG TCGTAACAAGG-3′) and ITS4 (5′-TCCTCCGCTTATTGATATGC-3′). PCR reactions (20 µL) contained 2 µL 10× Taq PCR buffer, 1.6 µL 2.5 mM dNTP mixture, 1 µL of each primer (10 pmol/µL), 1–2 µL template DNA (20 ng/µL), 0.2 µL KOMA-Taq DNA polymerase (2.5 U/µL), and nuclease-free water to volume. Cycling conditions were: 95 °C for 5 min; 30 cycles of 95 °C for 30 s, 55 °C for 2 min, and 68 °C for 1.5 min; final extension at 68 °C for 10 min; hold at 4 °C. Two isolates (K3.1.2 and M6.0.1) were processed at Genetika Science, Indonesia, for D1/D2 domain sequencing using NL1 (5′-GCATATCAATAAGCGGAGGAAAAG-3′) and NL4 (5′-GGTCCG TGTTTCAAGACGG-3′). PCR reactions (25 µL) contained 12.5 µL MyTaq™ HS Red Mix (2×; Bioline, UK), 1 µL of each primer (10 µM), ~ 50 ng genomic DNA, and nuclease-free water. Cycling conditions were: 95 °C for 1 min; 35 cycles of 95 °C for 10 s, 52 °C for 15 s, and 72 °C for 15 s; hold at 4 °C. PCR products were purified and sequenced bidirectionally (Macrogen Inc. for ITS; 1 st BASE, Singapore for NL). Resulting sequences were analyzed using BLASTn against the NCBI nucleotide database for species-level identification. For phylogenetic analysis, reference sequences were retrieved from GenBank and aligned with the study isolates in MEGA version 10.2.6 using the ClustalW algorithm with default parameters. Phylogenetic trees were generated using the maximum likelihood method, and branch support was assessed by bootstrap analysis[33].

Characterization of functional capabilities related to polyethylene biodegradation

PE degradation potential test on solid media

The yeast isolates were cultivated on a mineral medium composed of (per L): 3 g NH_4NO_3, 5 g K_2HPO_4, 1 g NaCl, 0.2 g $MgSO_4 \cdot 7\ H_2O$, and 15 g agar. This medium was supplemented with 10 g L^{-1} polyethylene (PE) powder[28] and 0.05% Tween80 to aid dispersion, achieved by vortexing for 1 min. The cultures were incubated at 30 °C[34]. Following incubation for 7 to 14 days. The yeast isolates that exhibited growth indicating potential PE degradation[28]. To further confirm degradation activity, a qualitative clear zone assay was performed on mineral salt agar (same basal composition) supplemented with 10 g L^{-1} powdered PE (sterilized by immersion in 70% ethanol for 1–2 h, followed by UV exposure for 30 min) and 0.25 mL L^{-1} Tween 20. Yeast isolates were spot-inoculated and incubated for 7–14 days. Plates were then flooded with 0.1% (w/v) Coomassie Brilliant Blue, incubated for 20 min, and destained for 25 min. The presence of a clear halo surrounding the colony indicated extracellular enzymatic activity capable of degrading PE particles embedded in the agar matrix. Halo diameters were measured as previously described[27], and newly acquired representative photographs are presented alongside the corresponding measurements in Supplementary Figure S6.

Biofilm formation

The biofilm formation potential of yeast isolates on PE was assessed using crystal violet staining. Biofilms were developed under static conditions, with yeast suspensions prepared by resuspending several loops of yeast isolate in sterile 0.85% physiological saline until an optical density (OD) of 0.5 at 600 nm was reached. Subsequently, 1.2 mL of the suspension was added to a 6-well cell culture plate containing 3 ml of Bushnell-Haas (BH) medium and sterilized 5 × 5 mm PE coupons (previously treated with 70% ethanol for 20 min and air-dried). The BH medium composition included (per L) 1.0 g NH_4NO_3, 0.2 g $MgSO_4 \cdot 7\ H_2O$, 1.0 g K_2HPO_4, 0.1 g $CaCl_2 \cdot 2\ H_2O$, and 0.15 g KCl, supplemented with 30 g L^{-1} NaCl. The negative control consisted of sterile medium containing the PE coupons without microbial inoculation, incubated under the same conditions as the test samples. After 7 days, the coupons were rinsed twice with 0.1 mol L^{-1} phosphate buffer (pH 7.4) to remove non-adherent cells. Biofilms were stained by adding 500 µL of 0.1% crystal violet solution to each coupon, incubating for 45 min at room temperature (26 °C). Excess dye was removed by washing the coupons three times with 1 mL of sterile water.The bound crystal violet was then solubilized using 500 µL of 95% ethanol, incubated for 30 min at 4 °C. A 100 µl sample from each well was transferred to a 96-well microtiter plate, and OD was measured at 595 nm using iMark Microplate Absorbance Reader (Bio-Rad). The OD cutoff value (ODc) was calculated as the mean OD of the negative control plus three times its standard deviation (SD). This ODc is used to minimize the influence of non-specific or background staining—such as residual crystal violet that may remain on the plastic surface even in the absence of yeast[35]. The ODc was determined to be 0.0549. Biofilm formation was classified as follows: non-adherent (OD ≤ ODc), weakly adherent (ODc < OD ≤ 2xODc), moderately adherent (2xODc < OD ≤ 4xODc), and strongly adherent (4xODc < OD)[36,37]. Biofilm formation was assessed in three independent

biological replicates. Data are presented as mean ± standard deviation (SD), with SD values shown as error bars in the corresponding figure.

PE degradation by single-culture yeast in liquid medium

The inoculum was prepared by transferring several loops of yeast culture into 0.85% (w/v) physiological saline and adjusting the suspension to an OD_{600} of 0.5 using a spectrophotometer. A 10% (v/v) inoculum of this OD_{600}-adjusted suspension was then used for the assay[11,38,39] and 0.2% polyethylene (PE) pellets[40] were added into 100 mL of Bushnell-Haas (BH) medium. The mixture was incubated at room temperature (26 °C) in a shaker incubator set to 150 rpm for 10 days[41]. A control treatment without yeast inoculation was also included. All treatments were conducted in triplicate. The effectiveness of the biodegradation process was evaluated by measuring the dry weight reduction of the PE sample using the following formula[39]:

$$Weight\ reduction\ (\%) = \frac{Initial\ weight - Final\ weight}{Initial\ weight} x100$$

The culture was filtered, and the polyethylene granules were soaked in 2% sodium dodecyl sulfate (SDS) for 4 h, followed by rinsing with distilled water and oven-drying at 60 °C[42,43]. The dry weight loss of the plastic was determined by calculating the difference between the initial and final dry weights before and after biodegradation.

Morphological changes resulting from the polymer biodegradation assay were examined on samples that exhibited the most effective degradation using a Scanning Electron Microscope (SEM) SU3500 at a magnification of up to 10,000x. Changes in functional groups were analyzed by Fourier Transform Infrared (FTIR) spectroscopy using an IR Prestige-21 spectrophotometer (Shimadzu, Japan) operated in % transmittance mode over the range 400–4000 cm^{-1}, with a resolution of 4 cm^{-1} and 50 scans per sample. Polyethylene (PE) pellets were finely ground with an agate mortar and pestle, then homogenized with spectroscopic-grade potassium bromide (KBr) that had been oven-dried for 24 h to remove moisture. The mixture was placed in a KBr die and compressed at 10 tons to produce a transparent pellet. A blank KBr pellet was scanned as the background. Spectra were baseline-corrected and smoothed (smoothing factor 5–12) using IR Solution software (Shimadzu) prior to analysis.

Carbon source utilization profile using biolog EcoPlate™

The yeast isolate with the highest polyethylene (PE)–degrading activity was pre-cultured in half-strength Wickerham's YM medium supplemented with 0.25% n-hexadecane until the mid-logarithmic phase (≈ 10^8 cells mL^{-1}). Cells were harvested (8,000 × g, 15 min), washed twice with 1× phosphate-buffered saline (PBS), and resuspended to an OD_{600} of 1.0 (≈ 10^8 cells mL^{-1}). A 100 µL aliquot of this suspension was inoculated into each well of a Biolog EcoPlate™. Plates were incubated in the dark at 37 °C for 5 days. Well absorbance (OD_{590}) was measured daily (days 0–5). For each substrate, OD values were corrected by subtracting the corresponding water-control well; negative values were set to zero before data aggregation. The heatmap shows the mean OD of three technical replicates per substrate, with corresponding standard deviations provided in Supplementary Table S3. EcoPlate profiling was conducted from a single independent culture (three technical replicates per substrate) and is presented descriptively; no statistical hypothesis testing was performed.

Biosurfactant assay

The ability of yeast to produce biosurfactants was observed from the emulsification activity test. A 10% yeast inoculum (cell density ≈ 10^8–10^9 cells mL^{-1})[44] was grown in 180 mL of Bushnell-Hass medium supplemented with 2% crude oil. The culture was incubated at 150 rpm and room temperature (26 °C) for 4 days. Following incubation, the culture was centrifuged at 12,000 rpm for 30 min at 4 °C to obtain the cell-free supernatant for use in the biosurfactant assay[23]. The crude biosurfactant obtained from the supernatant was subsequently used to assess emulsification activity. The assay was performed by adding 2 mL of crude oil to a test tube containing 2 mL of the supernatant. The mixture was vortexed at high speed for 2 min and left for 24 h. The emulsification index (EI_{24}) was determined in two independent biological replicates. Results are expressed as mean ± SD, with SD values shown as error bars in the corresponding figure. The percentage of emulsification value (EI_{24}) was calculated based on the following Eqs[45,46].:

$$\mathrm{EI}_{24}\% = \frac{emulsified\ layer\ height}{total\ liquid\ column\ height} \times 100$$

Genomic analysis

Genomic DNA extraction, library preparation, and whole genome sequencing (WGS)

The yeast isolates with the highest PE biodegradation potential were subjected to whole-genome sequencing (WGS). Genomic DNA (gDNA) of the isolate was extracted using Quick-DNA Magbead Plus Kit (Zymoresearch, D4082)[47], which then subjected to initial quantification and purity observation with Nanodrop 2000 (Thermo Scientific), DNA visualization with Agarose Gel Electrophoresis, accurate quantification with Qubit dsDNA HS Assay Kits (Thermo Scientific), and integrity with 4150 TapeStation (Agilent). Total gDNA was used for the input of library preparation. Library Prep Kit using xGen DNA Library Prep EZ UNI Kit (IDT, 10009822). The gDNA was fragmented using enzymatic methods to match the expected insert size. The fragmented DNA was ligated with Illumina-compatible Adapter with unique index for each sample. PCR was conducted to amplify the library. The quality and quantity of library samples were determined using Tape Station and Qubit Fluorometer, respectively. Sequencing was conducted 300 cycles (PE150) using Illumina NextSeq 2000 (Genetika Science Lab, Tangerang, Indonesia). Filtering was performed using fastp. Filtered reads were used for de novo[48].

Genome assembly and annotation

De novo genome assembly was performed using SPAdes v4.0.0[49]. The assembly quality was assessed with QUAST v5.3.0[50] and BUSCO v5.8.2[51]. Repeat regions in the genome were identified using RepeatModeler v2.0.5[52] and subsequently masked with RepeatMasker v4.1.5[53]. Gene prediction was conducted using BRAKER v3.0.8[54] with the --fungus option. Transfer RNAs (tRNAs) and ribosomal RNAs (rRNAs) were identified using tRNAscan-SE v1.3.1[55] and Barrnap v0.9 (https://github.com/tseemann/barrnap), respectively. All predicted genes were annotated using multiple databases, including Clusters of Orthologous Groups (KOG) (http://www.ncbi.nlm.nih.gov/COG), Kyoto Encyclopedia of Genes and Genomes (KEGG) (https://www.kegg.jp)[56,57], Swiss-Prot, TrEMBL (https://www.uniprot.org/uniprotkb), and the Non-Redundant (NR) protein database (https://ftp.ncbi.nlm.nih.gov/blast/db/.). Functional annotation was performed using DIAMOND blastp v2.1.8[58]. Based on NR database annotations, Gene Ontology (GO) (http://www.ebi.ac.uk/GOA) were assigned using Blast2GO[59]. Protein family classification was performed using the Pfam database (http://pfam.xfam.org/) with HMMER v3.3.2[60].

Visualization of genome

Visualization was generated using Circos v0.69.8[61].

Phylogenomics analysis

The genomes of species from the *Meyerozyma guilliermondii* complex and *Clavispora lusitaniae* were retrieved from NCBI with the GenBank assembly accessions as follows: M. *guilliermondii*: GCA_000149425.1, GCA_900174495.1, *M. caribbica*: GCA_000755205.1, GCA_900231965.1, GCA_900232065.1, *M. carpophila*: GCA_001599235.1, *C. lusitaniae*: GCA_000003835.1. OrthoFinder v3.0.1b1 was used to identify orthogroups[62]. Single-copy orthogroups (SCOs), defined as orthogroups with exactly one protein in all samples, were selected for phylogenomic analysis. Each SCO was aligned using MUSCLE v5.1[63], and recombination was assessed with PhiPack v1.1[64]. An SCO was considered nonrecombinant if it passed all three recombination tests in PhiPack. Nonrecombinant SCO alignments were refined using Gblocks v0.91b[65] and concatenated with a custom Python script. The final concatenated alignment was used as input for RAxML v8.2.12[66] under the PROTCAT approximation, applying the LG substitution model with 1000 bootstrap replicates.

Results

Morphological characteristics and identification of yeast

Yeast morphological characterization was performed macroscopically by colonies and microscopically by cells based on Kurtzman and Fell characterization[67] (Supplementary Table S1). Supplementary Figure S1 presents macroscopic and microscopic morphological features of the isolates. The results show that each isolate exhibited distinct morphological characteristics.

The BLAST analysis results of ITS and D1/D2 (Supplementary Table S2) identified isolates BI.4.1.1 and K3.1.2 as *Rhodotorula mucilaginosa* with identity values of a 100% and 99.49%, respectively. Isolate M5.0.1 was identified as *Candida tropicalis* with 100% identity, while isolate M5.0.3 was determined to be *Crinitomyces flavificans* also with 100% Identity. Isolate M6.0.1 was confirmed as *Moesziomyces antarcticus* with a 100% Identity. Additionally, isolate M6.0.2 was identified as *Meyerozyma carpophila* with an Identity value of 99.81%. The resulting sequences of BI.4.1.1, K3.1.2, M.5.0.1, M.5.0.3, M.6.0.1, and M.6.0.2 were deposited in GenBank under the accession numbers PV596362, PV596366, PV596363, PV596364, PV596367, and PV596365,respectively.

The internal transcribed spacer (ITS) region and the D1/D2 domain of the 26 S rDNA were selected for molecular identification. Representative sequences from related yeasts were retrieved from the GenBank database to serve as reference points for comparison. These sequences and those obtained from the isolates in this study were aligned and used to construct phylogenetic trees using the MEGA-X software. Phylogenetic analysis was conducted to determine the evolutionary relationships and confirm the taxonomic placement of the isolates (Supplementary Figure S2-S4).

Characterization of functional capabilities related to polyethylene biodegradation

Potential of yeast for PE degradation observed on solid media

Supplementary Figure S5 compares the growth of yeast isolates on Wickerham's YM medium and mineral salt medium containing polyethylene (PE) powder. All yeast isolates formed colonies on mineral salts agar supplemented with polyethylene (PE) powder within 10 days of streak inoculation, indicating growth under PE-containing conditions. Qualitative halo formation was observed for a subset of isolates, with diameters summarised in Supplementary Figure S6. The largest halo was recorded for isolate M5.0.1 (~ 1 mm; adapted from Alami et al.[27]), whereas M5.0.3 showed no detectable halo under these conditions. Halo size is reported as a descriptive indicator of surface-associated activity on PE agar; no statistical analysis was performed.

Biofilm formation

The results of the biofilm formation assay are presented in Fig. 1. All isolates exhibited the ability to form biofilms, with M6.0.1 and M5.0.1 showing intermediate biomass, while BI.4.1.1, K3.1.2, M6.0.2, and M5.0.3 were classified as weak biofilm producers based on OD600 values. Biofilm data did not follow a normal distribution according to the Kolmogorov–Smirnov test; therefore, statistical comparisons were performed using the Mann–Whitney U test. Isolate M6.0.2 exhibited significantly different biofilm biomass than BI.4.1.1 ($p = 0.050$), K3.1.2 ($p = 0.050$), M6.0.1 ($p = 0.050$), and the control ($p = 0.050$), while no significant differences were observed compared to M5.0.1 ($p = 0.513$) or M5.0.3 ($p = 0.513$).

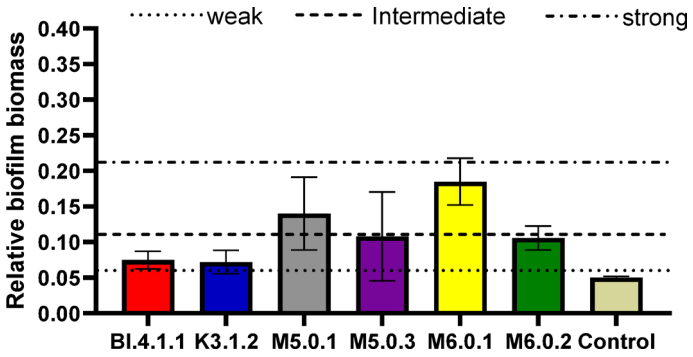

Fig. 1. Biofilm formation by yeast isolates on polyethylene (PE) surfaces is illustrated, with the y-axis representing the mean Optical Density (OD) values at 590 nm across three replicates per isolate. Horizontal lines indicate cutoff values for categorizing biofilm formation strength as weak, intermediate, or strong. Isolates are classified as follows: nonadherent, $OD \leq ODc$ (0.0549); weakly adherent, $ODc < OD \leq 2 \times ODc$; moderately adherent, $2 \times ODc < OD \leq 4 \times ODc$; and strongly adherent, $OD > 4 \times ODc$. The OD cutoff value (ODc) was determined as the mean OD of the negative control plus three times the standard deviation.The negative control consisted of PE incubated in sterile medium without yeast inoculation. Error bars represent the standard deviation from three independent biological replicates.

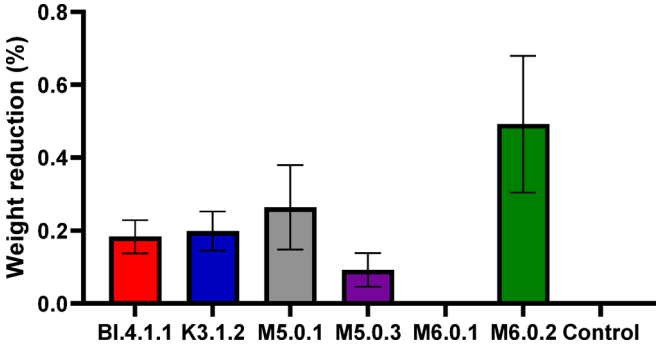

Fig. 2. Weight reduction percentage of polyethylene after 10 days of incubation. The experiment was conducted under an initial pH of approximately 7, agitation at 150 rpm, and a temperature of 26 °C, using three independent biological replicates for each treatment. Error bars indicate standard deviation of the mean. The control consisted of PE incubated in sterile medium without yeast inoculation.

PE degradation by single-culture yeast in liquid medium

The experimental results for each isolate cultured in Bushnell-Haas liquid medium, incubated for 10 days with the addition of 0.2% polyethylene (PE) (< 5 mm in size), are visualized in Figs. 2. These results are based on the percentage reduction in PE dry weight.

As shown in Fig. 2, among all tested isolates, M6.0.2 exhibited the highest mean percentage of PE dry weight reduction. Independent Samples t-test analysis revealed that M6.0.2 differed significantly from the control ($p = 0.045$) and from M6.0.1 ($p = 0.045$), while differences with other isolates were not statistically significant ($p > 0.05$). M6.0.2 consistently achieved the highest degradation values across replicates, supporting its selection for further analyses.

Fourier Transform Infrared (FTIR) Spectroscopy was employed to analyze chemical changes in the PE structure resulting from the degradation process. Figure 3 shows the FTIR spectra of the PE samples treated with isolate M6.0.2 alongside the untreated control (without yeast inoculum).

The FTIR spectrum of PE degraded by isolate M6.0.2 showed clear differences from the control (Fig. 3). New absorption bands were detected at ~ 3425 cm^{-1} (O–H stretching) and ~ 1651 cm^{-1} (C = O stretching), both of which are widely recognized as signatures of oxidative degradation in polyethylene. The presence of these functional groups indicates that oxidative processes, most likely mediated by microbial enzymes, contributed to the chemical alterations in the polymer backbone.

Chemical alterations in the surface morphology of PE were further investigated using SEM. The control PE sample (Fig. 4D and E, and 4F), exhibited a smooth and intact surface prior to biodegradation. In contrast, the PE samples treated with isolate M6.0.2 showed evident surface alterations, as illustrated in Fig. 4A and B, and C, captured at magnifications of 1000x, 5000x, and 10,000x, respectively.

To further investigate the metabolic profile of strain M6.0.2, additional testing was performed using Biolog ECOPlates. As shown in Supplementary Figure S7 and Supplementary Table S3, strain M6.0.2 exhibited active

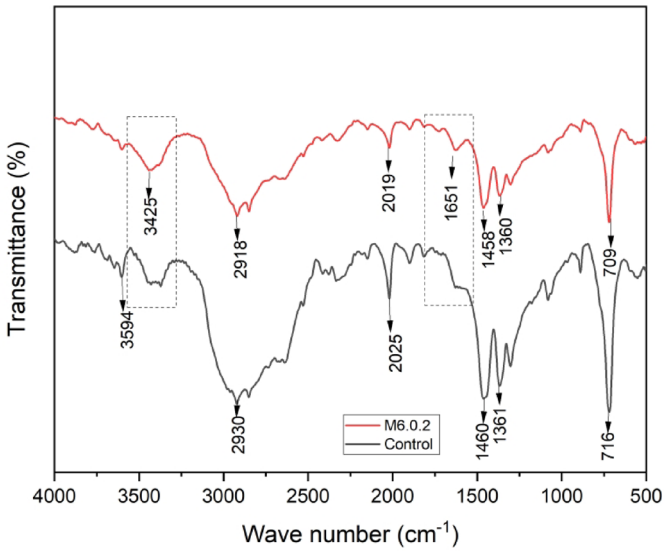

Fig. 3. FT-IR spectra of polyethylene pellets for sample M6.0.2 and control.

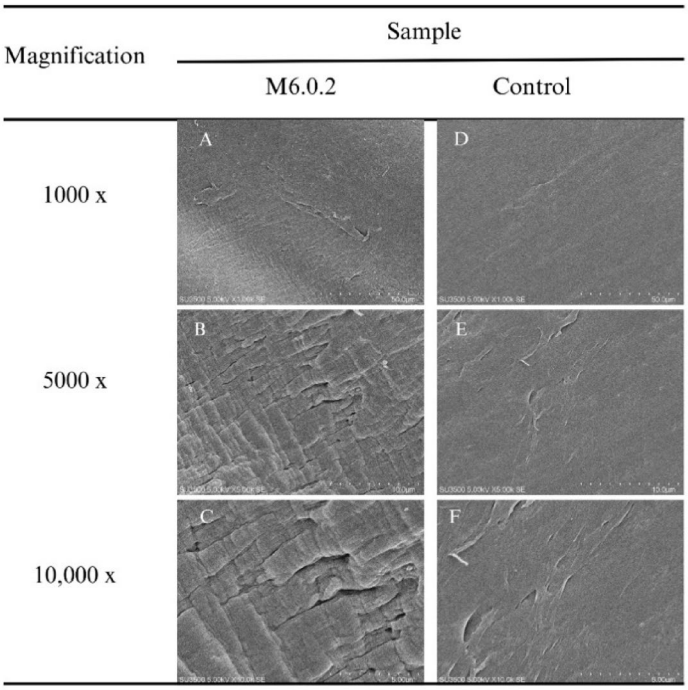

Fig. 4. Surface topography of PE pellets observed by SEM: (A) and (D) M6.0.2 and control, respectively, at 1000× magnification (scale bar: 50 µm); (B) and (E) M6.0.2 and control at 5000× magnification (scale bar: 10 µm); (C) and (F) M6.0.2 and control at 10,000× magnification (scale bar: 5 µm). Scale bars are located at the bottom of each image.

growth and demonstrated the ability to assimilate a wide range of substrates. Notably, it was also able to utilize several analog hydrocarbon substrates, such as Tween 40 and Tween 80, as well as their metabolic intermediates, including itaconic acid, pyruvic acid methyl ester, and 2-/4-hydroxybenzoic acid.

To complement these findings, the emulsification index was measured to determine whether isolate M6.0.2 possesses biosurfactant-producing capabilities, which may contribute to the PE degradation process. The results, indicating biosurfactant production by isolate M6.0.2, are shown in Supplementary Figure S8. The results of the emulsification test (Supplementary Figure S8) showed the ability of strain M6.0.2 to emulsify crude oil starting at 24 h, with a notable increase observed between 48 and 72 h, after which the activity stabilized. Meanwhile, the pH was known to decrease until the 72 h, followed by a gradual increase toward the end of the incubation period.

Genome assembly and annotation

Next, the best isolate, M6.0.2, exhibited PE degradation ability, was subjected to Whole Genome Sequencing (WGS) using the Illumina NextSeq 2000 (PE 150) platform to obtain a comprehensive overview of its genomic structure. After genome assembly, correction, and optimization, a total sequence length of 10,339,184 bp was assembled into 108 contigs with an N50 length of 1,078,351 bp. The GC content of the assembled contig was 47.32%. M6.0.2 genome includes 5,352 coding protein genes, and the average length of protein-coding genes was 1,754.76 bp. In addition, the non-coding RNA, including four rRNA and 145 tRNA, was predicted (Table 1). The average coverage depth was 621x and complete BUSCO was 96.4%. The predicted result of the total repeated sequence length was 107,940 bp, covering 1.04% of the genomic length.

Genome functional annotations of the 5352 predicted protein-coding genes using the public databases of GO, KEGG, KOG, Pfam, SwissProt, TrEMBL and NR. The protein-coding genes were annotated in the GO database, which were divided into three major classes and 48 functional groups (Supplementary Figure S9A). Among them,21, 14 and 13 subclasses exist in the biological process, cellular component, and molecular function and biological process, respectively. The classification chart of the KEGG pathways is shown in Supplementary Figure S9B. Among the KEGG pathways, signal transduction (645 genes), transport and catabolism (499 genes) and carbohydrate metabolism (425 genes) have more abundant gene numbers than other pathways. In addition, Supplementary Figure S9C shows genes annotated in the KOG database. Based on the figure, the largest number of genes (1345) are from the function unknown category, followed by other categories such as Intracellular trafficking, secretion, and vesicular transport (489) and Post-translational modification, protein turnover, and chaperons (453).

To align the genome analysis with the study's focus on polyethylene (PE) degradation, we curated a representative subset of PE-relevant genes into a simplified functional table (Table 2) grouped by enzymatic role, while the complete locus-level annotation remains available in Supplementary Table S4. The table highlights peroxidases implicated in polymer oxidation—laccase (e.g., g689.t2), glutathione peroxidase—together with non-heme chloroperoxidase (e.g., g4974.t1). Candidates for initial hydroxylation of reduced PE fragments are represented by CYP52-family P450s (e.g., CYP52A12 g2834.t1, CYP52A13 g1257.t1). Downstream conversion includes alcohol dehydrogenase (e.g., g2038.t1) and aldehyde dehydrogenase (e.g., g64.t1), followed by esterase/lipase (e.g., g773.t1, g2076.t2) and entries consistent with fatty acyl–CoA processing/β-oxidation (e.g., acyl-CoA thioesterase 9 g3612.t1; peroxisomal acyl-CoA thioester hydrolase 1 g3705.t1). Table 2 lists representative IDs per category to retain readability; full database hits and additional loci are provided in Supplementary Table S4 (with KEGG category counts in Supplementary Table S5).

Visualization of genome

Finally, a detailed circular genome diagram of M6.0.2 is displayed in Fig. 5. The outermost circle is labeled with the size of the genome, and each scale is 50 Kb. From the outside to the inside (Fig. 5A), the second and third loops represent the characteristics of the whole genome, including the positive chain gene and negative chain gene, where different colors represent different COG/KOG functional classifications (Fig. 5B). The fourth and fifth loops exhibited the ncRNA, including rRNA (green) and rRNA (pink). The sixth circle is the GC content; the outward black part indicates that the GC content in this region is higher than the average GC content in the

Parameter	Value
Genome assembly	
Contigs number	108
GC content (%)	47.32
N50 (bp)	1,078,351
N90 (bp)	319,671
L50	4
Gap ratio (%)	0.00
Coding ratio (%)	79.85
Gene prediction and analysis	
Genome size (bp)	10,339,184
Number of protein-coding genes	5,352
Gene total length (bp)	8,609,179
Gene average length (bp)	1,754.76
CDSs total length (bp)	8,255,479
CDSs number	9,151
Exon length (bp)	8,257,946
Intron length (bp)	459,533
Repeated sequence percentage (%)	1.04
rRNA number	4
tRNA number	145

Table 1. General features associated with the genome in *Meyerozyma carpophila* M6.0.2.

Category	Key enzymes	Representative locus IDs	Role in PE pathway	Evidence tags (KO/PFAM)
Peroxidase—laccase (multicopper oxidase)	Laccase abr2	g689.t2	Oxidative modification of polymer surface; promotes carbonyl/hydroxyl introduction	PF07732.21; Cu-oxidase_3
Peroxidase—glutathione peroxidase	Glutathione peroxidase; Peroxiredoxin HYR1	g2936.t1, g2936.t4	Oxidative support and peroxide reduction during polymer oxidation	KO: K23856; PF00255.25; GSHPx
Peroxidase—non-heme chloroperoxidase	Non-heme chloroperoxidase	g4974.t1	Haloperoxidase-type oxidative reactions contributing to polymer oxidation	PF00561.26; Abhydrolase_1
Alkane monooxygenase (or functional analog: CYP52)	Cytochrome P450 52A13; Cytochrome P450 52A12	g1257.t1, g2834.t1	Initial hydroxylation of reduced PE fragments (ω/terminal) yielding alcohols	PF00067.27; p450
Alcohol dehydrogenase	NADP-dependent alcohol dehydrogenase 6	g2038.t1, g2224.t2	Alcohol →aldehyde conversion	KO: K00002; K05351; PF08240.17; ADH_N
Aldehyde dehydrogenase	mitochondrial aldehyde dehydrogenase; putative oxidoreductase	g64.t1, g65.t1	Aldehyde →carboxylic acid conversion	KO: K00128; PF00171.27; PF00106.31; Aldedh; adh_short
Esterase/lipase	Sterol esterase TGL1; putative lipase	g773.t1, g2076.t2	Hydrolysis of ester products to acids and alcohols	KO: K01052; PF04083.22; PF01764.32; Abhydro_lipase; Lipase_3
β-oxidation/fatty acyl—CoA processing	Peroxisomal acyl-coenzyme A thioester hydrolase 1; Acyl-coenzyme A thioesterase 9 mitochondrial	g3705.t1, g3612.t1	Channeling fatty acids into β-oxidation toward central metabolism	KO: K17361; PF20789.3; 4HBT_3C

Table 2. Selected polyethylene (PE)-associated genes identified in *Meyerozyma Carpophila* M6.0.2, grouped according to predicted enzymatic function.

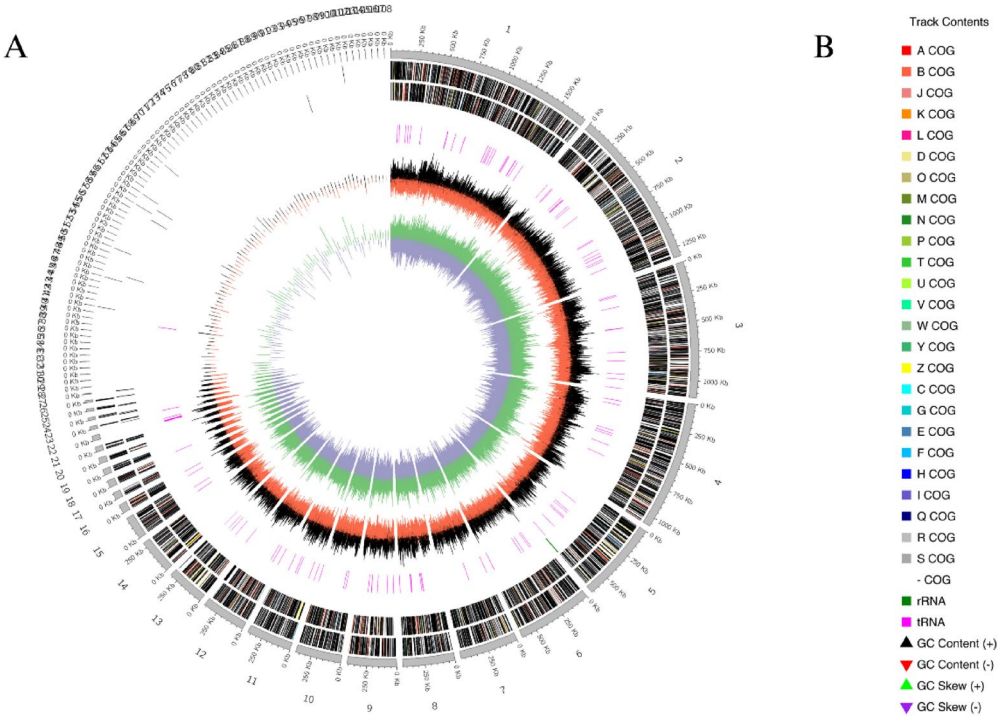

Fig. 5. The *Meyerozyma carpophila* M6.0.2 circular genome diagram. (**A**) The circular genome diagram. (**B**) The COG/KOG functional classification in circular diagram.

genome. The higher the peak value, the more significant the difference from the average GC content. The inward orange part is the opposite. The innermost layer is the GC skew (the specific algorithm: G-C/G + C), where the outward green part indicates that the C content in this area is lower than that of G, and the inward blue part is the opposite.

We retrieved 1,135 SCOs, which were then aligned with MUSCLE and tested for recombination with PhiPack. We retained 695 nonrecombining SCOs and processed their MSAs with Gblocks. The polished MSAs were concatenated, obtaining a 310,003 bp long alignment. We used this final MSA as input for RAxML, obtaining a phylogenetic tree with 100% bootstrap support for all branches (Fig. 6). Four evident clades can be seen in the tree, which is *Clavispora lusitaniae* as the outermost single species clade, and the genomes of M6.0.2 clustering together with *M. carpophila* clade.

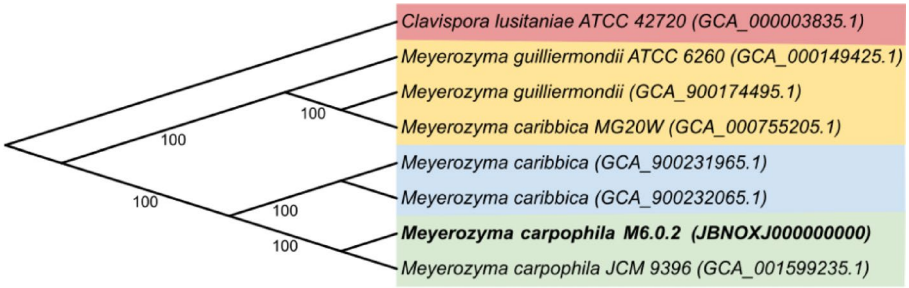

Fig. 6. Maximum likelihood tree. Resulting clades are highlighted: *M. guilliermondii* (yellow), *M. caribbica* (blue), *M. carpophila* (green), and *C. lusitaniae* (red).

Comparative genomic analysis between isolate M6.0.2 and other related strains (Supplementary Table S6) revealed notable differences based on orthogroup analysis. Thus, it shows that M6.0.2 can be considered a new strain of *Meyerozyma carpophila*.

Discussion

The BLAST analysis results of ITS and D1/D2 (Supplementary Table S2) revealed that isolates BI.4.1.1 and K3.1.2 were identified as *Rhodotorula mucilaginosa*. This species has been documented as a marine yeast capable of degrading polyethylene (PE). This was demonstrated through the experiment, UV-irradiated ^{13}C-labeled polyethylene, resulting in a degradation rate of 3.8% per year[22]. Isolate M5.0.1 was identified as *Candida tropicalis*. According to Zahari et al.[68] *C. tropicalis* was capable of degrading low-density polyethylene (LDPE) film by up to 3.2% after a 7-week incubation period, using a 10% culture inoculum. Isolate M5.0.3 was identified as *Crinitomyces flavificans*. To date, no studies have reported the potential of *C. flavificans* for plastic degradation. Isolate M6.0.1 showed a match to the species *Moesziomyces antarcticus*. Several species within this genus have demonstrated biological activity against biodegradable plastics (BPs) and for the production of biosurfactants with various industrial applications[69]. Furthermore, isolate M6.0.2 was identified as *Meyerozyma carpophila*. This species was initially named *Candida guilliermondii var. carpophila* in 1961 and later renamed *Candida carpophila* in 2005. Based on recent molecular analysis, this species is more appropriately placed in the genus *Meyerozyma*, which is now named *Meyerozyma carpophila*. This species belongs to the Guilliermondii complex, a group of phylogenetically related yeasts with similar morphological characteristics. In addition to *M. carpophila*, the Guilliermondii complex group includes other species, such as *Meyerozyma guilliermondii*, *Meyerozyma caribbica*, and *Candida glucosophila*[70,71]. *M. carpophila* is a yeast that is not yet known to have a sexual (teleomorphic) phase in its life cycle, unlike some other yeasts that have two phases: asexual (anamorphic) and sexual (teleomorphic)[72]. This yeast can grow in 10% NaCl. In biodegradation research using seawater media, salt resistance is an important indicator. Moreover, *M. carpophila* possesses lipase enzymes, which may play a significant role in the polyethylene degradation process[70].

To date, no studies have revealed the role of *Meyerozyma carpophila* in polyethylene (PE) degradation. However, one study from the genus Meyerozyma reported on *M. caribbica*, which has demonstrated notable potential for low-density polyethylene (LDPE) degradation. A 45-day incubation period with the addition of Tween 80 resulted in a 13.3% reduction in LDPE dry weight. Moreover, enzyme activity assays confirmed the presence of laccase, manganese peroxidase (MnP), and lignin peroxidase (LiP) in the degradation medium[18,24].

Figure 1 shows that all yeast isolates were capable of forming biofilms. According to Gilan et al.[21], microbial degradation of solid polymers such as PE requires biofilm formation, as microorganisms must attach to and colonize the PE surface for effective degradation[21].Therefore, biofilm formation is considered essential in plastic degradation. However, the ability of yeast to form biofilms must be further evaluated through degradation assays, as not all microbes capable of forming biofilms possess the ability to degrade plastic[73].

As shown in Fig. 2, the study incorporated abiotic factors such as elevated temperatures and ultraviolet (UV) radiation to address this challenge. Prior to the experiment, the PE granules were pretreated by soaking in alcohol for 2 h, followed by drying in an oven at 50 °C for approximately two nights. Additionally, the granules were exposed to UV radiation for 1 h. This pretreatment induces oxidative damage, facilitating subsequent enzymatic oxidation by various enzymes secreted by yeast[74–76]. UV radiation has a complex impact on the biodegradation of plastic. It can induce either main-chain cleavage, cross-linking, or a combination of both[77].

Based on Fig. 1, all yeast isolates demonstrated the ability to form biofilms, which was supported by applying abiotic treatments, including elevated temperature and UV radiation. These treatments contributed to the biodeterioration phase, which compromised the structural integrity of PE and reduced its dry weight, as shown in Fig. 2.

Determination of the dry weight loss is a simple and rapid method for assessing the biodegradation of polymers or plastics. This method correlates with the formation of biofilms on the plastic surface and within its cracks, which leads to the loss of the physical integrity of PE and contributes to its dry weight reduction. The extent of weight loss is generally proportional to the surface area, as biodegradation typically begins at the polymer surface in a process referred to as biodeterioration[43,78].

The FTIR spectrum of PE degraded by isolate M6.0.2 (Fig. 3) revealed the appearance of distinct absorption bands at ~ 3425 cm^{-1} and ~ 1651 cm^{-1}. Signals within the 1700–1650 cm^{-1} region are typically associated

with carbonyl groups such as aldehydes and ketones, which are frequently detected as intermediates during polyethylene biodegradation[79]. The band near 3425 cm^{-1} reflects O–H stretching vibrations, consistent with the formation of hydroxyl-containing compounds such as alcohols or phenolic derivatives[33]. The occurrence of these oxygenated functional groups is in line with enzymatic oxidation processes, often mediated by microbial oxidases (e.g., laccases and peroxidases) and oxygenases (e.g., alkane hydroxylases), which introduce oxygen atoms into otherwise inert hydrocarbon backbones. Collectively, these spectral changes support the interpretation that extracellular enzyme activity played a central role in driving the chemical modifications observed in degraded PE[80,81].

The treated PE pellets (Fig. 4) exhibited a rough and uneven surface, characterized by pronounced cavities and substantial morphological alterations compared to the control samples. These surface irregularities may indicate an enhanced affinity of the tested yeast isolate toward the PE substrate[30].

Based on the results of the ECOPlates assay (Supplementary Figure S7 and Supplementary Table S3), a marked increase in optical density (OD) was observed for nearly all substrates beginning at 24 h of incubation. This trend suggests that the yeast exhibits rapid growth and high metabolic activity across a broad range of carbon sources provided in the ECOPlate. Notably, several substrates potentially linked to polyethylene degradation—including hydrocarbon analogs such as Tween 40 and Tween 80, along with metabolic intermediates such as itaconic acid, pyruvic acid methyl ester, and 2-/4-hydroxybenzoic acid—elicited consistently high metabolic responses throughout the incubation period[82].

To date, enzymes involved in polyethylene degradation have been primarily linked to hydrocarbon-degrading pathways. These pathways typically involve a series of oxidative enzymes, such as laccases, peroxidases, and monooxygenases[83], alongside hydrolytic enzymes like lipases and esterases, which possess broad substrate specificity[84,85]. In the context of Biolog ECOPlates, several substrates act as analogs or metabolic intermediates relevant to polyethylene degradation. Specifically, Tween 40 and Tween 80 serve as hydrocarbon analogs and are widely used to assess lipase activity due to their esterified oleic acid content, which is preferentially hydrolyzed by lipases[86,87]. Moreover, the ability of the isolate to metabolize intermediates such as itaconic acid, pyruvic acid methyl ester, and 2-/4-hydroxybenzoic acid reflects the activity of core metabolic pathways, including those involved in fatty acid and aromatic compound catabolism—processes commonly associated with both hydrocarbon and polyethylene degradation[82].

Enzymes—particularly oxidative enzymes involved in PE degradation—typically function by breaking down the polymer into smaller, esterified compounds through stepwise chemical reactions. Additionally, hydrolases such as lipases and esterases can catalyze the hydrolysis of ester bonds, resulting in the formation of new functional groups such as carboxylates and hydroxyls[25]. The incorporation of these functional groups enhances the hydrophilic properties of the PE surface[88].

Yeasts often display hydrophobic cell surfaces due to protein-rich walls; however, these proteins are not always exposed, and hydrophilic fibrils may mask them depending on growth conditions, producing shifts between hydrophobic and hydrophilic phenotypes[89,90]. Consistent with this plasticity, across isolates, dry-weight loss did not scale with total biofilm biomass (Figs. 1 and 2). Notably, the top-degrading isolate, M6.0.2, produced the greatest dry-weight loss despite forming only a weak biofilm. Prior studies similarly indicate that while biofilm facilitates initial colonization on hydrophobic substrates such as PE, larger biofilm biomass does not necessarily imply higher degradation[73].

These observations suggest that interfacial properties of the biofilm at the polymer–liquid boundary, rather than bulk biomass, better explain the observed dry-weight loss. During early attachment, yeasts secrete extracellular polymeric substances (EPS)—a predominantly hydrophilic matrix of polysaccharides, proteins, lipids, and DNA—that modulates cell-surface properties and interactions at the interface[91,92]. Matrix porosity, local oxygen and enzyme diffusion, and interfacial wetting are therefore likely to govern sustained contact with PE and the extent of dry-weight loss under our conditions[93,94]. In line with this view, M6.0.2 exhibited emulsification (Supplementary Fig. S8), compatible with biosurfactant production. Biosurfactants reduce interfacial tension; their hydrophobic moieties can associate with the polymer while hydrophilic headgroups engage the aqueous phase, increasing PE wettability and access for cells and enzymes[95]. Although emulsification was not measured concurrently with the dry-weight-loss assay, its presence in the highest-degrading isolate aligns with a qualitative link between biosurfactant-mediated wetting and enhanced processing of a hydrophobic surface. Finally, pH is a key determinant of biosurfactant production and performance: most yeasts grow optimally at pH 4–6, and pH shifts can alter biosurfactant morphology and solubility, thereby modulating interfacial activity[96,97].

The raw sequencing data, including the N50 value of 1,078,351 bp, indicated the median contig length (Table 1). These data indicate that contigs of this length or longer covered at least 50% of the assembled genome. This metric is often used as an indicator of genome assembly quality. During the de novo assembly process, the reads were assembled into a single contig with a length of approximately 1,731,636 bp, which reflects the final assembled genome size. The GC content of the M6.0.2 isolate genome was 47,32%. This percentage reflects the guanine (G) and cytosine (C) bases in the genome and is often used to assess genomic characteristics such as genome stability or environmental adaptation. This value is in line with the standard GC content range for yeast and may provide insight into this isolate's biological or ecological properties[98].

The completeness of the assembled genome was assessed using the BUSCO method. The results of the BUSCO evaluation of isolate M6.0.2 showed a gene completeness level of 96.2%, with 3,608 complete genes identified from the total analyzed. These genomic features indicate that the assembly process was successful, yielding a complete genome with a consistent GC content and a high degree of gene completeness[98].

The annotation results revealed that the genome of M6.0.2 harbors genes encoding enzymes related to polyethylene degradation. To make the link between genome annotation and PE degradation explicit, we summarize representative genes by enzymatic role in Table 2, while the complete locus-level annotation is available in Supplementary Table S4 (KEGG category counts in Supplementary Table S5)[56,57].

The proposed degradation pathway is illustrated in Supplementary Figure S10. Several peroxidases, including laccase, glutathione peroxidase, and non-heme chloroperoxidase, are involved in PE degradation, which can lead to a decrease in the molecular weight of PE and ultimately destroy the PE polymer through oxidation. Carbonyl groups may be introduced along the polymer backbone during this oxidative process. The reduced PE molecules can be recognized as intermediate products and/or substrates for alkane monooxygenase to produce alcohol compounds, which can then be oxidized to aldehyde by alcohol dehydrogenases. Aldehydes produced during metabolism can be oxidized to carboxylic acids by aldehyde dehydrogenase. In addition, ester products can be hydrolyzed carboxylic acids and alcohols by esterase or lipase. Finally, fatty acids taken up by cells enter the β-oxidation pathway; the resulting compounds can then be used as metabolites and carbon sources (as well as CO_2 and H_2O) during mineralization. Although multiple enzyme classes are involved in PE degradation, complete breakdown of the polymer is challenging for a single enzyme due to the stability of successive alkane (C – C) bonds. Therefore, future research should prioritize the identification and development of a consortium of enzymes capable of collaboratively degrading polyethylene[25,81,99].

Conclusion

This study successfully isolated and identified yeasts from marine plastic debris obtained from selected coastal sites in East Java, Indonesia. *Meyerozyma carpophila* M6.0.2 exhibited the highest polyethylene (PE)-degrading potential, as evidenced by a 0.4923% reduction in PE dry weight, visible alterations on the PE surface, and the formation of new functional groups—including aldehydes, ketones, and alcohols—after 10 days of incubation. The isolate was also capable of forming biofilms and producing biosurfactants, both of which can facilitate the biodegradation process. Whole-genome sequencing further revealed the presence of key genes encoding enzymes associated with PE degradation, including peroxidase, cytochrome P450 monooxygenase, alcohol dehydrogenase, aldehyde dehydrogenase, lipase, and esterase. The results of this study indicate that *Meyerozyma carpophila* M6.0.2 can degrade PE based on its functional and genomic characteristics, highlighting its potential for application in plastic waste bioremediation.

Data availability

The *Meyerozyma carpophila* M6.0.2 BioSample and BioProject are available at DDBJ/ENA/GenBank under the accession numbers SAMN48324007 and PRJNA1258570, respectively. The Whole Genome Shotgun project has been deposited at DDBJ/ENA/GenBank under the accession JBNOXJ000000000. The version described in this paper is version JBNOXJ010000000.

Received: 5 June 2025; Accepted: 3 October 2025
Published online: 18 November 2025

References

1. Yu, R. S., Yang, Y. F. & Singh, S. Global analysis of marine plastics and implications of control measure strategies. *Front. Mar. Sci.* **10**, (2023).
2. Oliveira, J. et al. Marine environmental plastic pollution: mitigation by microorganism degradation and recycling valorization. Frontiers in Marine Science vol. 7 Preprint at (2020). https://doi.org/10.3389/fmars.2020.567126
3. Thushari, G. G. N. & Senevirathna, J. D. M. Plastic pollution in the marine environment. Heliyon vol. 6 Preprint at (2020). https://doi.org/10.1016/j.heliyon.2020.e04709
4. Debroy, A., George, N. & Mukherjee, G. Role of biofilms in the degradation of microplastics in aquatic environments. Journal of Chemical Technology and Biotechnology vol. 97 3271–3282 Preprint at (2022). https://doi.org/10.1002/jctb.6978
5. Kögel, T., Bjorøy, Ø., Toto, B., Bienfait, A. M. & Sanden, M. Micro- and nanoplastic toxicity on aquatic life: Determining factors. Science of the Total Environment vol. 709 Preprint at (2020). https://doi.org/10.1016/j.scitotenv.2019.136050
6. Kale, S. K., Deshmukh, A. G., Dudhare, M. S. & Patil, V. B. Microbial degradation of plastic: a review. *J. Biochem. Technol.* **6**, 952–961 (2015).
7. Tokiwa, Y., Calabia, B. P., Ugwu, C. U. & Aiba, S. Biodegradability of plastics. International Journal of Molecular Sciences vol. 10 3722–3742 Preprint at (2009). https://doi.org/10.3390/ijms10093722
8. Zadjelovic, V. et al. A mechanistic Understanding of polyethylene biodegradation by the marine bacterium alcanivorax. *J. Hazard. Mater.* **436**, (2022).
9. Sari, D. A. A., Suryanto, Sudarwanto, A. S., Nugraha, S. & Utomowati, R. Reduce marine debris policy in Indonesia. in iop conference series: earth and environmental science vol. 724IOP Publishing Ltd, (2021).
10. Wang, Y. & Karasik, R. *Policy Brief Plastic Pollution Policy Country Profile: Indonesia. NI PB 22 – 05* (Duke University, 2022).
11. Shao, H. et al. Complete genome sequence and characterization of a polyethylene biodegradation strain, streptomyces albogriseolus LBX-2. Microorganisms 7, (2019).
12. El-Shafei, H. A., El-Nasser, A., Kansoh, N. H., Ali, A. M. & A. L. & Biodegradation of disposable polyethylene by fungi and streptomyces species. *Polym. Degrad. Stab.* **62**, 361–365 (1998).
13. Zeenat, Elahi, A., Bukhari, D. A., Shamim, S. & Rehman, A. Plastics degradation by microbes: A sustainable approach. Journal of King Saud University - Science vol. 33 Preprint at (2021). https://doi.org/10.1016/j.jksus.2021.101538
14. Miri, S. et al. Biodegradation of microplastics: Better late than never. Chemosphere vol. 286 Preprint at https://doi.org/ (2022). https://doi.org/10.1016/j.chemosphere.2021.131670
15. Srikanth, M., Sandeep, T. S. R. S., Sucharitha, K. & Godi, S. Biodegradation of plastic polymers by fungi: a brief review. Bioresources and Bioprocessing vol. 9 Preprint at (2022). https://doi.org/10.1186/s40643-022-00532-4
16. Yao, Z., Seong, H. J. & Jang, Y. S. Environmental toxicity and decomposition of polyethylene. Ecotoxicology and Environmental Safety vol. 242 Preprint at (2022). https://doi.org/10.1016/j.ecoenv.2022.113933
17. Abdel-Motaal, F. F., El-Sayed, M. A., El-Zayat, S. A. & Ito, S. ichi. Biodegradation of Poly (ε-caprolactone) (PCL) film and foam plastic by *pseudozyma Japonica* sp. nov., a novel cutinolytic ustilaginomycetous yeast species. *3 Biotech.* **4**, 507–512 (2014).
18. Elsamahy, T., Sun, J., Elsilk, S. E. & Ali, S. S. Biodegradation of low-density polyethylene plastic waste by a constructed tri-culture yeast consortium from wood-feeding termite: degradation mechanism and pathway. *J. Hazard. Mater.* **448**, (2023).
19. Vaksmaa, A., Hernando-Morales, V., Zeghal, E. & Niemann, H. Microbial degradation of marine plastics: current state and future prospects. in biotechnology for sustainable environment 111–154Springer Singapore, (2021). https://doi.org/10.1007/978-981-16-1955-7_5

20. Sarkar, S., Pramanik, A., Mitra, A. & Mukherjee, J. Bioprocessing data for the production of marine enzymes. Marine Drugs vol. 8 1323–1372 Preprint at (2010). https://doi.org/10.3390/md8041323
21. Gilan, I. & Sivan, A. Effect of proteases on biofilm formation of the plastic-degrading actinomycete *Rhodococcus ruber* C208. *FEMS Microbiol. Lett.* **342**, 18–23 (2013).
22. Vaksmaa, A. et al. Polyethylene degradation and assimilation by the marine yeast *Rhodotorula mucilaginosa*. *ISME Commun.* **3**, (2023).
23. Kavitha, R. & Bhuvaneswari, V. Assessment of polyethylene degradation by biosurfactant producing ligninolytic bacterium. *Biodegradation* **32**, 531–549 (2021).
24. Ali, S. S. et al. Coupling Azo dye degradation and biodiesel production by manganese-dependent peroxidase producing oleaginous yeasts isolated from wood-feeding termite gut symbionts. *Biotechnol. Biofuels* **14**, (2021).
25. Seo, M. J., Yun, S., Do, Kim, H. W. & Yeom, S. J. Polyethylene-biodegrading microbes and their future directions. biotechnology and bioprocess engineering vol. 28 977–989 Preprint at (2023). https://doi.org/10.1007/s12257-022-0264-9
26. Da Costa, J. P. et al. Degradation of polyethylene microplastics in seawater: insights into the environmental degradation of polymers. *J. Environ. Sci. Health Tox Hazard. Subst. Environ. Eng.* **53**, 866–875 (2018).
27. Alami, N. H. et al. Biodegradation of low-density polyethylene (LDPE) using yeast isolates from plastic waste biofilms. *Sains Malays.* **54**, 1739–1750 (2025).
28. Brunner, I., Fischer, M., Rüthi, J., Stierli, B. & Frey, B. Ability of fungi isolated from plastic debris floating in the shoreline of a lake to degrade plastics. *PLoS One* **13**, (2018).
29. Zhang, C. et al. Assembly strategies for polyethylene-degrading microbial consortia based on the combination of omics tools and the plastisphere. *Front. Microbiol.* **14**, Preprintathttpsdoiorg103389fmicb20231181967 (2023).
30. Fotopoulou, K. N. & Karapanagioti, H. K. Surface properties of beached plastic pellets. *Mar. Environ. Res.* **81**, 70–77 (2012).
31. Ting, A. S. Y. & Sallahudin, A. Y. Biodegradation potential of mixed cultures of *Bacillus* sp. and Priestia sp. from landfill investigated on Low-Density polyethylene (LDPE) sheets. *Water Air Soil. Pollut* **236**, (2025).
32. Kutty, S. N. & Philip, R. Marine yeasts - A review. Yeast vol. 25 465–483 Preprint at (2008). https://doi.org/10.1002/yea.1599
33. Ojha, N. et al. Evaluation of HDPE and LDPE degradation by fungus, implemented by statistical optimization. *Sci. Rep.* **7**, (2017).
34. Zampolli, J. et al. Transcriptomic analysis of *Rhodococcus opacus* R7 grown on polyethylene by RNA-seq. *Sci. Rep.* **11**, (2021).
35. O'Toole, G. A. Microtiter dish biofilm formation assay. *J. Visualized Experiments*. https://doi.org/10.3791/2437 (2010).
36. Jang, Y. et al. Biofilm characteristics for providing resilient denitrification in a hydrogen-based membrane biofilm reactor. *Water Res.* **231**, (2023).
37. Bumunang, E. W., Ateba, C. N., Stanford, K., McAllister, T. A. & Niu, Y. D. Biofilm formation by South African non-o157 Shiga toxigenic *Escherichia coli* on stainless steel coupons. *Can. J. Microbiol.* **66**, 328–336 (2020).
38. Fibriarti, B. L. & Feliatra, Amin, B. Darwis. Biodegradation of Ldpe plastic by local strain of *Bacillus* sp. Isolated from dump soil of pekanbaru, Indonesia. *Biodiversitas* **22**, 5484–5490 (2021).
39. Kyaw, B. M., Champakalakshmi, R., Sakharkar, M. K., Lim, C. S. & Sakharkar, K. R. Biodegradation of low density polythene (LDPE) by Pseudomonas species. *Indian J. Microbiol.* **52**, 411–419 (2012).
40. Bhatia, M., Girdhar, A., Tiwari, A. & Nayarisseri, A. Implications of a novel Pseudomonas species on low density polyethylene biodegradation: an in vitro to in Silico approach. *Springerplus* **3**, (2014).
41. Khandare, S. D., Chaudhary, D. R. & Jha, B. Marine bacterial biodegradation of low-density polyethylene (LDPE) plastic. *Biodegradation* **32**, 127–143 (2021).
42. Gilan, I., Hadar, Y. & Sivan, A. Colonization, biofilm formation and biodegradation of polyethylene by a strain of *Rhodococcus ruber*. *Appl. Microbiol. Biotechnol.* **65**, 97–104 (2004).
43. Das, M. P. & Kumar, S. An approach to low-density polyethylene biodegradation by *Bacillus amyloliquefaciens*. *3 Biotech.* **5**, 81–86 (2015).
44. Ibrahim, S. et al. Biosurfactant production and growth kinetics studies of the waste Canola oil-degrading bacterium *Rhodococcus erythropolis* AQ5-07 from Antarctica. *Molecules* **25**, (2020).
45. Katemai, W. Biosurfactants from yeasts. *Walailak J.* **9**, 1–8 (2011).
46. da Silva, A. F., Banat, I. M., Giachini, A. J. & Robl, D. Fungal biosurfactants, from nature to biotechnological product: bioprospection, production and potential applications. Bioprocess and Biosystems Engineering vol. 44 –2034 Preprint at (2003). https://doi.org/10.1007/s00449-021-02597-5 (2021).
47. Zymo Research. Quick-DNA™ MagBead Plus kit rapid high-throughput method for DNA isolation from any sample. Instruction Manual. (2023).
48. Sevim, V. et al. Shotgun metagenome data of a defined mock community using Oxford Nanopore, PacBio and illumina technologies. *Sci. Data* **6**, (2019).
49. Bankevich, A. et al. SPAdes: A new genome assembly algorithm and its applications to single-cell sequencing. *J. Comput. Biol.* **19**, 455–477 (2012).
50. Gurevich, A., Saveliev, V., Vyahhi, N. & Tesler, G. Quast: quality assessment tool for genome assemblies. *Bioinformatics* **29**, 1072–1075 (2013).
51. Simão, F. A., Waterhouse, R. M., Ioannidis, P., Kriventseva, E. V. & Zdobnov, E. M. BUSCO: assessing genome assembly and annotation completeness with single-copy orthologs. *Bioinformatics* **31**, 3210–3212 (2015).
52. Flynn, J. et al. Ten things you should know about transposable elements 06 biological sciences 0604 genetics. *Genome Biol.* **19**, (2018).
53. Tarailo-Graovac, M. & Chen, N. Using repeatmasker to identify repetitive elements in genomic sequences. *Curr. Protocols Bioinf. Preprint at.* https://doi.org/10.1002/0471250953.bi0410s25 (2009).
54. Hoff, K. J., Lomsadze, A., Borodovsky, M. & Stanke, M. Whole-genome annotation with BRAKER. in Methods in Molecular Biology vol. 65–95 (Humana Press Inc., 2019). (1962).
55. Chan, P. P., Lin, B. Y., Mak, A. J. & Lowe, T. M. TRNAscan-SE 2.0: improved detection and functional classification of transfer RNA genes. *Nucleic Acids Res.* **49**, 9077–9096 (2021).
56. Kanehisa, M. & Goto, S. K. E. G. G. Kyoto encyclopedia of genes and genomes. *Nucleic Acids Res.* **28** (2000). http://www.genome.ad.jp/kegg/
57. Kanehisa, M., Furumichi, M., Sato, Y., Matsuura, Y. & Ishiguro-Watanabe, M. Kegg: biological systems database as a model of the real world. *Nucleic Acids Res.* **53**, D672–D677 (2025).
58. Buchfink, B., Xie, C. & Huson, D. H. Fast and sensitive protein alignment using Diamond. Nature Methods vol. 12 59–60 Preprint at (2014). https://doi.org/10.1038/nmeth.3176
59. Conesa, A. et al. Blast2GO: A universal tool for annotation, visualization and analysis in functional genomics research. *Bioinformatics* **21**, 3674–3676 (2005).
60. Finn, R. D., Clements, J. & Eddy, S. R. Hmmer web server: interactive sequence similarity searching. *Nucleic Acids Res.* **39**, (2011).
61. Krzywinski, M. et al. Circos: an information aesthetic for comparative genomics. *Genome Res.* **19**, 1639–1645 (2009).
62. Emms, D. M., Kelly, S. & OrthoFinder Phylogenetic orthology inference for comparative genomics. *Genome Biol.* **20**, (2019).
63. Edgar, R. C. & Muscle A multiple sequence alignment method with reduced time and space complexity. *BMC Bioinform.* **5**, (2004).
64. Bruen, T. & PhiPack *Phi Test and Other Tests of Recombination* (McGill University, Montreal, 2005).
65. Talavera, G. & Castresana, J. Improvement of phylogenies after removing divergent and ambiguously aligned blocks from protein sequence alignments. *Syst. Biol.* **56**, 564–577 (2007).

66. Stamatakis, A. Raxml version 8: A tool for phylogenetic analysis and post-analysis of large phylogenies. *Bioinformatics* **30**, 1312–1313 (2014).
67. Kurtzman, C. P., Fell, J. W. & Boekhout, T. The Yeasts. vol. 5 (2010).
68. Zahari, N. Z., Abdullah, S. N., Tuah, P. M. & Cleophas, F. N. Biodegradation of low-density polyethylene (LDPE) and starch – based plastic (SBP) by thermophiles *Bacillus subtilis* and *Candida tropicalis*. *IOP Conf. Ser. Mater. Sci. Eng.* **1173**, 012035 (2021).
69. Liu, Y., Zou, Z., Hu, Z., Wang, W. & Xiong, J. Morphology and molecular analysis of *Moesziomyces antarcticus* isolated from the blood samples of a Chinese patient. *Front. Microbiol.* **10**, (2019).
70. Kurtzman, C., Fell, J. W. & Boekhout, T. *The Yeasts A Taxonomic Study* 5th Edn (Elsevier, 2011).
71. Vaughan-Martini, A., Kurtzman, C. P., Meyer, S. A. & O'Neill, E. B. Two new species in the *Pichia guilliermondii* clade: *Pichia caribbica* sp. Nov., the Ascosporic state of *Candida fermentati*, and *Candida Carpophila* comb. Nov. *FEMS Yeast Res.* **5**, 463–469 (2005).
72. de Marco, L. et al. The genomes of four *Meyerozyma caribbica* isolates and novel insights into the *Meyerozyma guilliermondii* species complex. *G3: Genes Genomes Genet.* **8**, 755–759 (2018).
73. Delacuvellerie, A., Cyriaque, V., Gobert, S., Benali, S. & Wattiez, R. The plastisphere in marine ecosystem hosts potential specific microbial degraders including *alcanivorax borkumensis* as a key player for the low-density polyethylene degradation. *J. Hazard. Mater.* **380**, (2019).
74. Andrady, A. L. Microplastics in the marine environment. marine pollution bulletin vol. 62 1596–1605 Preprint at (2011). https://doi.org/10.1016/j.marpolbul.2011.05.030
75. Alami, N. H., Zulaika, E. & Shovitri, M. *Laporan Akhir Penelitian Prototipe Dana ITS 2020 Marine Yeast Potensial Pendegradasi Polimer Plastik Yang mengambang di lingkungan laut*. Institut Teknologi Sepuluh Nopember (2020).
76. Zhang, Y., Pedersen, J. N., Eser, B. E. & Guo, Z. Biodegradation of polyethylene and polystyrene: From microbial deterioration to enzyme discovery. Biotechnology Advances vol. 60 Preprint at (2022). https://doi.org/10.1016/j.biotechadv.2022.107991
77. Chandra, R. & Rustgi, R. B i o d e g r a d a b l e p o l y m e r s. *Prog Polym. Sci.* vol. 23 (1998).
78. Cheng, J. et al. Relative influence of plastic debris size and shape, chemical composition and phytoplankton-bacteria interactions in driving seawater plastisphere abundance, diversity and activity. *Front. Microbiol.* **11**, (2021).
79. Muhonja, C. N., Makonde, H., Magoma, G. & Imbuga, M. Biodegradability of polyethylene by bacteria and fungi from Dandora dumpsite Nairobi-Kenya. *PLoS One* **13**, (2018).
80. Zhang, F. et al. Current technologies for plastic waste treatment: A review. Journal of Cleaner Production vol. 282 Preprint at (2021).
81. Rong, Z., Ding, Z. H., Wu, Y. H. & Xu, X. W. Degradation of low-density polyethylene by the bacterium *Rhodococcus* sp. C-2 isolated from seawater. *Sci. Total Environ.* **907**, (2024).
82. Liu, H., Yang, G., Jia, H. & Sun, B. Crude oil degradation by a novel strain *Pseudomonas aeruginosa* AQNU-1 isolated from an oil-Contaminated. *Lake Wetland Processes* **10**, (2022).
83. Haritash, A. K. & Kaushik, C. P. Biodegradation aspects of polycyclic aromatic hydrocarbons (PAHs): A review. Journal of Hazardous Materials vol. 169 1–15 Preprint at (2009). https://doi.org/10.1016/j.jhazmat.2009.03.137
84. Abubakar, A., Abioye, O. P., Aransiola, S. A., Maddela, N. R. & Prasad, R. Crude oil biodegradation potential of lipase produced by *Bacillus subtilis* and *Pseudomonas aeruginosa* isolated from hydrocarbon contaminated soil. *Environ. Chem. Ecotoxicol.* **6**, 26–32 (2024).
85. Kadri, T. et al. Production and characterization of novel hydrocarbon degrading enzymes from *alcanivorax borkumensis*. *Int. J. Biol. Macromol.* **112**, 230–240 (2018).
86. Cai, Z. et al. Biological degradation of plastics and microplastics: a recent perspective on associated mechanisms and influencing factors. Microorganisms vol. 11 Preprint at (2023). https://doi.org/10.3390/microorganisms11071661
87. Putcha, J. P. & Kitagawa, W. Polyethylene biodegradation by an artificial bacterial consortium: *Rhodococcus* as a competitive plastisphere species. *Microbes Environ.* **39**, (2024).
88. Restrepo-Flórez, J. M., Bassi, A. & Thompson, M. R. Microbial degradation and deterioration of polyethylene - A review. International Biodeterioration and Biodegradation vol. 88 83–90 Preprint at (2014). https://doi.org/10.1016/j.ibiod.2013.12.014
89. Krasowska, A. & Sigler, K. How microorganisms use hydrophobicity and what does this mean for human needs? Frontiers in Cellular and Infection Microbiology vol. 4 Preprint at (2014). https://doi.org/10.3389/fcimb.2014.00112
90. Danchik, C. & Casadevall, A. Role of cell surface hydrophobicity in the pathogenesis of medically-significant fungi. frontiers in cellular and infection microbiology vol. 10 Preprint at (2021). https://doi.org/10.3389/fcimb.2020.594973
91. Babiak, W. & Krzemińska, I. Extracellular polymeric substances (EPS) as microalgal bioproducts: A review of factors affecting EPS synthesis and application in flocculation processes. Energies vol. 14 Preprint at (2021). https://doi.org/10.3390/en14134007
92. Li, Z., Li, H., Zhao, L., Liu, X. & Wan, C. Understanding the role of cations and hydrogen bonds on the stability of aerobic granules from the perspective of the aggregation and adhesion behavior of extracellular polymeric substances. *Sci. Total Environ.* **795**, (2021).
93. Flemming, H. C., Neu, T. R. & Wozniak, D. J. The EPS matrix: The 'House of biofilm cells'. Journal of Bacteriology vol. 189 7945–7947 Preprint at (2007). https://doi.org/10.1128/JB.00858-07
94. Stewart, P. S. et al. Reaction-diffusion theory explains hypoxia and heterogeneous growth within microbial biofilms associated with chronic infections. *NPJ Biofilms Microbiomes* **2**, (2016).
95. Ron, E. Z. & Rosenberg, E. Minireview natural roles of biosurfactants. *Environ. Microbiol.* **3** (2001).
96. Narendranath, N. V. & Power, R. Relationship between pH and medium dissolved solids in terms of growth and metabolism of lactobacilli and Saccharomyces cerevisiae during ethanol production. *Appl. Environ. Microbiol.* **71**, 2239–2243 (2005).
97. Abouseoud, M., Yataghene, A., Amrane, A. & Maachi, R. Effect of pH and salinity on the emulsifying capacity and naphthalene solubility of a biosurfactant produced by Pseudomonas fluorescens. *J. Hazard. Mater.* **180**, 131–136 (2010).
98. Wijayanti, C., Suryadarma, P. & Mubarik, N. R. Whole genome sequencing of a siderophore-producing bacterium isolated from Simadu pineapple roots. *Biodiversitas* **25**, 4860–4869 (2024).
99. Fukuda, R. & Ohta, A. Enzymes for aerobic degradation of alkanes in yeast. in Aerobic Utilization of hydrocarbons, Oils and Lipids 1–14 (Springer International Publishing, doi:https://doi.org/10.1007/978-3-319-39782-5_2-1. (2016).

Acknowledgements

This research was funded by Penelitian Pengabdian Masyarakat dan Inovasi (PPMI) SITH ITB 2025, Indonesia under the Collaborative Research Scheme.

Author contributions

N.H.A., F.P., I.A.P. and P.A. conceptualized and designed the research. N.H.A. and Z.R.P. performed the experiments, data analysis, and prepared the figures. F.P., I.A.P., P.A., T.E. and Y.S. supervised the work and edited the manuscript. All the authors read the present form of the manuscript and approved for submission.

Declarations

Competing interests
The authors declare no competing interests.

Additional information
Supplementary Information The online version contains supplementary material available at https://doi.org/10.1038/s41598-025-22911-5.

Correspondence and requests for materials should be addressed to T.E., I.A.P. or P.A.

Reprints and permissions information is available at www.nature.com/reprints.

Publisher's note Springer Nature remains neutral with regard to jurisdictional claims in published maps and institutional affiliations.